

PACKING MODELS OF YTTRIUM DOPED α - Al_2O_3 : STUDY OF POROSITY

N. Popescu-Pogrion^{*}, R. Bercia^a, M. Tirnovan^a

National Institute R&D of Materials Physics, 77125 Bucharest-Magurele, Romania

^aUniversity POLITEHNICA Bucharest, 313 Spl. Independentei, Bucharest, Romania

Dopant yttrium at 150 p.p.m. level (Y to Al atomic ratio) in ultra -high purity polycrystalline alumina has been found to be, together with the coefficient of porosity, the reason of grain growth : with abnormal grain growth (AGG) or with uniform grains. The powder, green bodies and sintering samples were studied by transmission electron microscopy (TEM), scanning electron microscopy (SEM), and packing models. In this paper we studied by mathematical modeling the correlation between structure of powder and green bodies in correlation with the porosity in sintering compacts. A formula, which describes the packing of the spherical - cylindrical homogeneous particles, has been obtained. The porosity of the low Y doped α - Al_2O_3 was investigated.

(Received April 20, 2004; accepted June 22, 2004)

Keywords: Porosity, α - Al_2O_3 , Packing modelling, Electron microscopy

1. Introduction

For sintered materials the micro-structural evolution depends on the characteristics of the starting powder (e.g., particle size, size distribution, particle shape and particle agglomerations); on the green compact microstructure (e.g., grain size, size distribution, grain shape, apparent porosity in green body) and on the sintering processes. During sintering, pores are removed from the ceramic body and grain boundaries develop between particles. If doping material is added, the doping ions may react with the major constituents and may be redistributed.

Krumov et al. [1] have shown that microstructural inhomogeneities of the Al_2O_3 samples influence the properties as: microhardness, thermal diffusion, refractive index. The characterisation of low Y doped α - Al_2O_3 powder materials used for the preparation of green body and sintered compact is one of the basic conditions for reaching the final desired properties. The shape, average size and homogeneity of the particles determine the structural characteristics of compact samples such as shape of grains, grain boundaries (GBs), surface and interfaces, porosity, phase separation. By mathematical modelling the correlation between the geometrical parameters of the powders, green bodies and sintering compacts has been studied.

In powder technology, packing models are of great importance for the structural properties of the green bodies and sintered compacts. In this paper we studied some structural and dimensional properties of low yttrium doped α - Al_2O_3 agglomerates: porosity, coefficient of porosity and packing, defined in quantified abstract space and real space R_3 . In the real space C. Gratson et al. [2], Y. Tokumitsu [4,5], I. J. Smaller [3], N.Popescu-Pogrion et al.[6,7], M.Tirnovan et al. [8], have been studied the packing types for spherical, ellipsoidal, cylindrical and prismatic uniform homogeneous particles [2 - 8]. We extended the theoretical packing models to the observed and measured particles with shapes typical for low Y (150 p.p.m.) doped alumina.

We used electron microscopy (transmission-TEM for initial powders and scanning-SEM for fractured and compact samples) and statistical determinations, to pick up information about the material - low Y doped α - Al_2O_3 .

* Corresponding author: pogrion@infim.ro

Dopant Y and residual impurities play a major role in determining the final microstructure and related properties of polycrystalline sintered alumina. In $\alpha\text{-Al}_2\text{O}_3$, the particular case of yttrium doping is interesting. Yttrium (Y) has a very limited solubility in $\alpha\text{-Al}_2\text{O}_3$ (10 p.p.m.). Due to the low solubility of Y in bulk $\alpha\text{-Al}_2\text{O}_3$, yttrium is strongly segregated at GB. They lead to strong modifications of the creep behaviour of pure alumina [9 - 11].

Yttrium doped $\alpha\text{-Al}_2\text{O}_3$ exhibits a creep resistance that is 1 to 2 orders of magnitude larger than that of the undoped ceramic. The creep is attributed to a suppression of grain boundary diffusion.

2. Experimental

The samples were prepared using a very pure AKP 3000 alumina powder as a starting material (with total cation impurity level less than 60 p.p.m.). There were prepared simultaneously two sets of samples, with low yttrium content (150 p.p.m.). The samples were sintered using two different sintering roads. One of them was adapted for the purpose to obtain porous samples (the Pp set of the samples) and the other was adapted to obtain compact ones (the Pc set samples). The Pp set of samples showed an average porosity of $\sim 2.8 (\pm 0.12) \%$ and the Pc set of samples showed a residual porosity of $\sim 0.04 (\pm 0.082) \%$. For both sets of samples, the alumina powder was mixed with an yttrium compound. Yttrium was added to the powders by the stoichiometric component $\text{Y}(\text{NO}_3)_3 \cdot 6\text{H}_2\text{O}$ (Strem Chem, Newburyport, MA).

The powder mixture was obtained and homogenised in a plastic mill in which the raw materials and Al_2O_3 balls were introduced in the following proportion: 1/3 powder: 1/3 alumina balls: 1/3 pure ethyl alcohol.

Two hours of mixing (homogenisation) was used for a perfect mixture. The mixture was filtered and dried, in high purity conditions, resulting a pure mixture of powders. The powder was ground for 10 minutes in an agate mortar and compacted by mechanical uniaxial pressing at 20 MPa, using a cylindrical mould, followed by an isostatic cold pressing at 800 MPa, for 1 minute.

Thus, the green body it was obtained. The SEM investigations made on that green body were correlated with the TEM investigations made on the initial powder, with the purpose to obtain an adequate relationship, which can describe the particle packing fitting the real conditions (regarding shape and the size distribution). The formula should express the porosity closer to the real value.

The samples were sintered following two different sintering cycles and then treated by annealing for 1-7 hours. The Pp set of samples was calcinated for 7 hours at 1100 °C (the heating rate was 5 °C/min) and then sintered for 2.5 hours at 1550 °C (the heating rate was 10°C/min for the interval 1100-1550 °C). The cooling rate was of about 38 °C/min. The Pc set of samples was sintered following a complex sintering curve, with intermediate steps.

The samples were cut in two equal pieces, perpendicular on the rotation axis of the cutting tool and thereafter polished. After the polishing there were made scanning microscopy tests (SEM on the polished samples, covered with a thin layer of gold, using a special installation of vaporisation). After the SEM, there were prepared the samples for the transmission electron microscopy, by ion milling. Grain size were determined by statistical methods in correlation with scanning electron microscopy investigations.

3. Packing and porosity in real geometric \mathbf{R}_3 space

Let the real geometric space with three dimensions be the set \mathbf{R}_3 endowed with structure $\text{St}(\mathbf{R}_3) = (\text{unit vector, hermitic structure, Hilbertian structure})$, a topological structure generated by an Euclidean metric total order structure, co-ordinates $f : \mathbf{R}_3 \rightarrow \mathbf{R}_3$ and a structure of quantification $q: P(\mathbf{R}_3) \rightarrow \mathbf{R}$. The q -quantified porosity of $B \subset \mathbf{R}_3$ related to a packing A is $g(B, A) = \{x, x \in (B - A)\}$.

If $C = \cup E_i \subseteq B$ thus so $\text{Fr}(B) \cap \text{Fr}(C) = \emptyset$ (therefore C is included in B) and, if B is a parallelepiped, then: i) B is an *elementary cell*; ii) C is *elementary particle* (grain);

If the geometric space \mathbb{R}_3 is endowed with the quantification $V : P(\mathbb{R}_3) \rightarrow \mathbb{R}$, where $V(B)$ is the volume of the domain $B \subset \mathbb{R}_3$, and B is an *elementary cell*, we define the coefficient of the porosity by

$$e_v(A, B) = \frac{V(B) - V(g(B, A))}{V(B)}$$

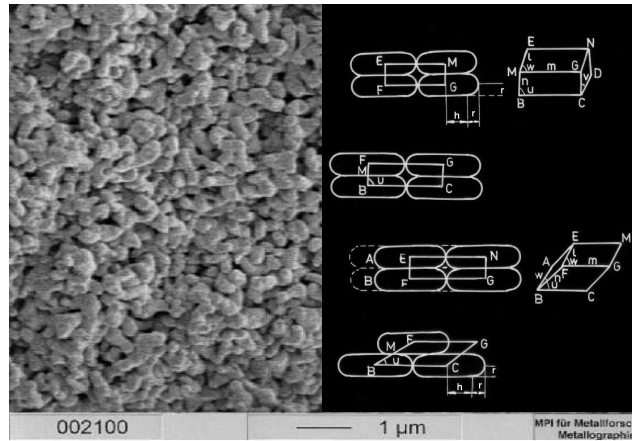


Fig. 1. Green body and elementary cell.

If the elementary cell $B(l, m, n) \subset \mathbb{R}_3$ is a parallelepiped defined by the vectors (l, m, n) then:

$$e_v = \frac{lmn(1 - \cos^2 u - \cos^2 v - \cos^2 w + 2 \cos u \cos v \cos w)^{1/2} - V(g(B, A))}{lmn(1 - \cos^2 u - \cos^2 v - \cos^2 w + 2 \cos u \cos v \cos w)^{1/2}}$$

where $u = \sphericalangle(l, n)$; $v = \sphericalangle(l, m)$; $w = \sphericalangle(m, n)$

If all particles from $H \subseteq \mathbb{R}_3$ have the same frontiers and the same volumes, then H is a domain with *homogeneous particles*. In [2 - 5] there were studied six packing types and also the adequate coefficient of porosity, for the domains with homogeneous spherical and elliptic particles. We consider the case of $H \subseteq \mathbb{R}_3$ that contains spherical-cylindrical-homogeneous particles, with radius r and cylindrical length $2h$. The coefficient of porosity in this case is

$$e = \frac{3lmn(1 - \cos^2 u - \cos^2 v - \cos^2 w + 2 \cos u \cos v \cos w)^{1/2} - 2\pi r^2(2r + 3h)}{3lmn(1 - \cos^2 u - \cos^2 v - \cos^2 w + 2 \cos u \cos v \cos w)^{1/2}}$$

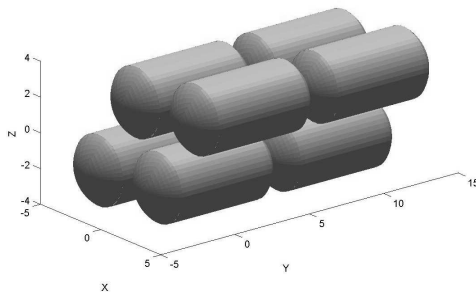


Fig. 2. Uniform packing with spherical-cylindrical particles.

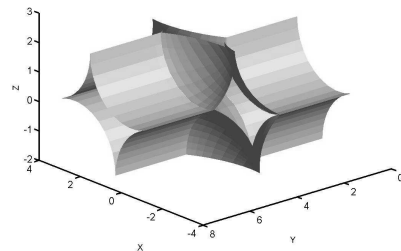


Fig. 3. Pore in an elementary cell.

The values of the porosity depend on the types of the packing (the values of $l, m, n, \cos u, \cos v, \cos w$ varying with r and h).

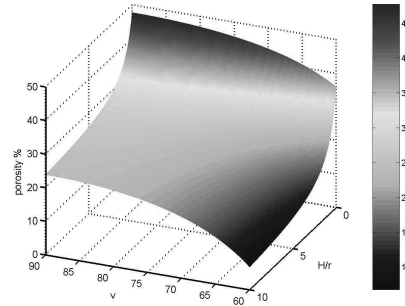
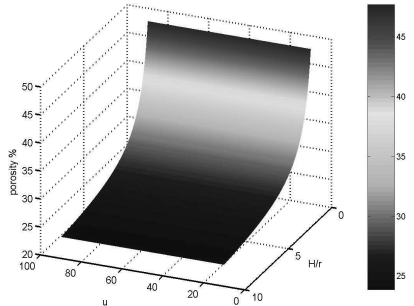


Fig. 4. Coefficient of porosity function of w and h/r . Fig. 5. Coefficient of porosity function of u and h/r .

Table 1. Value of coefficient of porosity function of the type of packing.

Type of packing	L	M	N	$\cos u$	$\frac{\cos v}{\cos w}$	e
1	$2r$	$2(r+h)$	$2r$	0	0	$\frac{2(6-\pi)r+3(4-\pi)h}{12(r+h)}$
2	$2r$	$2(r+h)$	$((r+h)^2+4r^2)^{1/2}$	$\frac{r+h}{((r+h)^2+4r^2)^{1/2}}$	0	$\frac{2(6-\pi)r+3(4-\pi)h}{12(r+h)}$

4. Results and discussion

The scanning electron microscopy pictures, histogram of the particle size distribution and mathematical packing models for initial powder, green body and sintered samples are presented in figures 1-7.

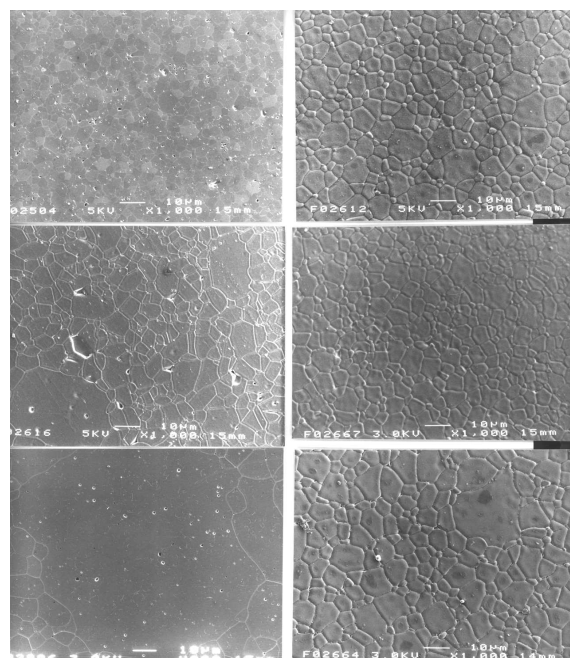
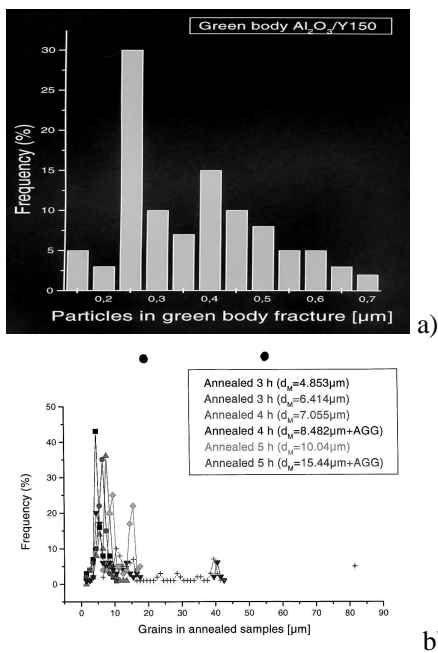


Fig. 6. Size distribution a) of green body particles, b) of sintered sample at different time of annealing.

Fig. 7. Variation of the grain size vs. annealing time at 1650°C . The evolution of samples ($P_p = 2.42\%$ and $P_c = 0.045\%$) as a function of annealing time (3h, 4h, 5h).

The packing model types are presented in Table 1 and Figures 1 - 5. The Fig. 6 a-b shows the dimensional distribution of grain size. The mean grain size for the green body is $0.388 \pm 0.1212 \mu\text{m}$.

Fig. 7 shows the scanning electron microscopy image of the samples. The microstructure of the 150 p.p.m. Y doped alumina samples at different annealing times (3h, 4h, 5h), in the case of two different porosities (Pp - porous and Pc - compact) is presented. All samples were sintered under identical conditions: 2 h30' at 1550 °C.

The very low porosity of Pc samples leads to an uniform growth and "fine" microstructure. The porous samples (Pp) present a bimodal grain size distribution with abnormal grain growth (AGG) (after 5h annealing). The grains are irregular in shape, but essentially isotropic.

5. Conclusions

This study reports the results obtained on the distribution and microstructure of initial powder, green body and sintered compacts (structure of the grains) in low Y doped α -alumina. The contribution of porosity in the evolution and development of the grains (especially in the development of the abnormal grain growth AGG) is evidenced. A new mode of growth was revealed for low porosity materials

Acknowledgements

We thanks Mrs. U. Salzberger for sample preparation, and Mrs. S. Kuhnemann for SEM assistance. The authors express the gratitude for financial support of MCT/PNCDI/CERES 3-114.

References

- [1] E. Krumow, V. Mankov, K. Starbova, J. Optoelectron. Adv. Mater. **5**(3), 675 (2003).
- [2] L. C. Gratson, H. J. Freser, J. Geol. **41**, 785 (1935).
- [3] I. J. Smaller, Powder Technology **4**, 97 (1970/71).
- [4] Y. Tokumitsu, J. Soc. Mater. Sci. Japan **13**, 732 (1964).
- [5] Y. Tokumitsu, Powder Technology **7**, 188 (1974).
- [6] N. Popescu-Pogrion, M. Tirnovan, V. Panaite, B. Nisipeanu, Proc. of Powder Metallurgy World Congress, Granada, Spain, 18-22 Oct.(1998), Vol.3, pp. 561.
- [7] N. Popescu-Pogrion, M. Tirnovan, S. Constantinescu, Proc., of European Conf. Advances in Hard Materials, Turin 141 (1999).
- [8] M. Tirnovan, R. Bercia, S. Constantinescu, N. Popescu-Pogrion. ICSS-12, NANO-8, June 28 - July 02. 2004, Venice, Italy.
- [9] Ian MacLaren, Mehmet A. Gulgun, Raissa Voythovych, Nicoletta Popescu-Pogrion, Ulrike Taffner, Rowland M. Cannon and Manfred Ruhle, J. Am. Ceram. Soc. **86**(4), (2003)
- [10] M. A. Gulgun, Manfred Ruhle, Key Engineering Materials Vols **171-174**, 793 (2000).
- [11] M. A. Gulgun, V. Putlayev, M. Ruhle, J. Am. Ceram. Soc. **82**(7), 1849 (1999).